International Journal of Pharmaceutics 423 (2012) 562–570

Contents lists available at SciVerse ScienceDirect

International Journal of Pharmaceutics

journal homepage: www.elsevier.com/locate/ijpharm

Pharmaceutical Nanotechnology

Functionalized (poly(ε-caprolactone))$_2$-poly(ethylene glycol) nanoparticles with grafting nicotinic acid as drug carriers

Jiraphong Suksiriworapong[a], Kittisak Sripha[b], Jörg Kreuter[c], Varaporn Buraphacheep Junyaprasert[a,*]

[a] Department of Pharmacy, Faculty of Pharmacy, Mahidol University, Bangkok 10400, Thailand
[b] Department of Pharmaceutical Chemistry, Faculty of Pharmacy, Mahidol University, Bangkok 10400, Thailand
[c] Institute of Pharmaceutical Technology, Goethe-University, Max-von-Laue-Str. 9 (Biozentrum), D-60438 Frankfurt am Main, Germany

ARTICLE INFO

Article history:
Received 16 September 2011
Received in revised form 30 October 2011
Accepted 23 November 2011
Available online 1 December 2011

Keywords:
Ibuprofen
Indomethacin
Nanoparticle
Nicotinic acid
Poly(ε-caprolactone)
Poly(ethylene glycol)

ABSTRACT

Nicotinic acid was grafted on (poly(ε-caprolactone))$_2$-poly(ethylene glycol) copolymers that were used for the preparation of nanoparticles with the objectives to monitor particle size and to optimize the drug loading capacity as well as the release profile of the particles. Increasing amounts of grafting nicotinic acid increased the particle size as a result of an enhanced hydrophobicity of the copolymer. Ibuprofen and indomethacin with two different molecular characteristics were selected as model drugs to be bound to the nanoparticles. The presence of grafting nicotinic acid enhanced the loading capacity for both drugs compared to the nanoparticles without nicotinic acid. However, no correlation between amount of grafting nicotinic acid and loading capacity was observed. The release characteristic of both drugs was fitted to the Higuchi model indicating Fickian diffusion. The release characteristic of indomethacin mainly depended on the crystalline property of the copolymer whereas that of ibuprofen was additionally influenced by the hydrogen bonding between drug and grafted copolymer.

1. Introduction

Poly(ε-caprolactone)-co-poly(ethylene glycol) copolymers (PCL-PEG) to be used as drug delivery systems in form of microparticles and nanoparticles have been employed and studied extensively (Zhou et al., 2003; Zhang et al., 2004; Vroman et al., 2007a; Huang et al., 2008; Gou et al., 2009; Lee et al., 2009; Nguyen and Nguyen, 2010). Owing to the amphiphilic properties of the copolymers, they showed advantages over PCL polymers such as the possibility for self assembly thus enabling an easy formation of particulate carriers. In addition, the presence of PEG in the polymer chain decreased uptake of the particles by the liver and kidney and prolonged retention in the blood (Hu et al., 2003; Zhang et al., 2004; Shenoy and Amiji, 2005; Zhang and Zhuo, 2005; Alexis et al., 2008; Chausson et al., 2008; Peng et al., 2008; Gou et al., 2009; Wei et al., 2009b). As a result, these PEGylated particles were used to encapsulate various kinds of drug, to improve drug action, to reduce unwanted side effects, or to offer controlled release (Wei et al., 2009a).

To increase the efficacy of the particles, certain functionalized polymers were synthesized (Trollsas et al., 2000; Lou et al., 2003; Vroman et al., 2007b; Riva et al., 2008). Functional groups that are attached to the polymer backbone may provide unique polymer characteristics thus directly influencing the polymer and nanoparticle properties (Sinko, 2006) as for example PEGylated poly(lactide) functionalized with carboxylic group (Lee et al., 2004) and polyphosphazenes functionalized with ethyl tryptophan (Zhang et al., 2006a), etc. In addition, not only the nature of carrier but also the molecular characteristics of bound drug can affect the properties of carriers, such as stability, drug loading capacity, drug entrapment efficiency, as well as their drug release profile (Sarisuta et al., 1999; Nair et al., 2001; Liu et al., 2004).

Non-steroidal anti-inflammatory drugs (NSAIDs) are one of the most widely used medicines for the treatment of osteoarthritis, rheumatoid arthritis, inflammations, and a variety of pains (Simon, 2002). The NSAIDs ibuprofen (IBU) and indomethacin (IND) possess different physicochemical characteristics concerning molecular structure, molecular size, and water-solubility. Because of their different properties these two drugs were chosen to investigate the compatibility and interaction with the copolymers which may be responsible for their loading and release characteristics. Their interaction with the polymer may involve van der Waals forces, dipole-dipole interaction, and hydrogen bonding (Van Krevelen and TeNijehuis, 2009).

Previously, the feasibility of grafting nicotinic acid (NI) and *p*-aminobenzoic acid on (poly(ε-caprolactone))$_2$-co-poly(ethylene glycol) copolymer ((PCL)$_2$-PEG) was investigated (Suksiriworapong et al., 2011). The properties of NI grafted copolymer ((P(NICL))$_2$-PEG) depended on the amounts of grafting NI on the copolymer.

* Corresponding author. Tel.: +66 2 644 8694; fax: +66 2 644 8694.
E-mail address: pyvbp@mahidol.ac.th (V.B. Junyaprasert).

0378-5173/$ – see front matter © 2011 Elsevier B.V. All rights reserved.
doi:10.1016/j.ijpharm.2011.11.033

In this study, the effect of NI grafted on $(PCL)_2$-PEG copolymers containing various amounts of grafting NI on nanoparticle formation and characteristics was investigated. The physicochemical properties of the resulting $(P(NICL))_2$-PEG nanoparticles with respect to particle size, morphology, surface charge, and toxicity were determined and compared with $(PCL)_2$-PEG nanoparticles. IBU and IND were chosen as model drugs and loaded at various drug to polymer ratios and the drug loading capacity, release characteristics, and possible interactions between drug and grafted copolymer were investigated.

2. Materials and methods

2.1. Materials

Nicotinic acid (NI) (Ajax Finechem, New South Wales, Australia) was used without purification. But-3-ynyl nicotinate was synthesized as previously reported (Suksiriworapong et al., 2010a). Azide-containing $(PCL)_2$-PEG copolymer ($(P(N_3CL))_2$-PEG) was manufactured according to a previously reported procedure (Suksiriworapong et al., 2011). Copper (I) iodide (CuI), 1,8-diazabicyclo[5.4.0]undec-7-ene (DBU), L-glutamine, and foetal bovine albumin serum (FBS) were purchased from Sigma–Aldrich Chemicals (Steinheim, Germany). MTT (3-(4,5-Dimethyl-2-thiazolyl)-2,5-diphenyl-2H-tetrazoliumbromide) was obtained from Fluka Chemie (Steinheim, Germany). Milli-Q water was used by purification with a Synergy® (Millipore, Molsheim, France). IMDM (Iscove's Modified Dulbecco Medium) was obtained from Biochrom AG (Berlin, Germany). Penicillin/streptomycin (Hoechst, Germany), sodium dodecyl sulphate (SDS) (MP Biochemicals, LLC, Heidelberg, Germany), trypsin (Difco, Germany), 100% acetic acid (VWR International S.A.S, Darmstadt, Germany), and other organic solvents were used as received. HUVECs (human umbilical vein endothelial cells) were isolated from human umbilical cord donated from Nordwest-Krankenhaus (Nordwest Hospital, Frankfurt, Germany). Acetonitrile and methanol from Merck (Darmstadt, Germany) were of HPLC grade. IBU and IND were a kind gift from Vita Co. Ltd. and Government of Pharmaceutical Organization (GPO) (Bangkok, Thailand).

2.2. Preparation and characterization of preformed PEGylated copolymers

NI was grafted on the $(P(N_3CL))_2$-PEG backbone by "click reaction" according to a previously published method (Suksiriworapong et al., 2010a, 2011). But-3-ynyl nicotinate was grafted at the azide position using CuI as a catalyst and DBU as a base. The grafting reaction was conducted at 40 °C for 4 h. The molar grafting was varied employing percentages of 10%, 20%, and 30% based on hydrophobic segments. $(PCL)_2$-PEG was synthesized by ring-opening polymerization at 120 °C for 24 h and used as a template copolymer for comparison. The obtained copolymers were characterized by gel permeation chromatography (GPC) using a Water 150-CV gel permeation chromatograph for the number- and weight-average molecular weights (M_n and M_w), respectively. The copolymer was eluted through a PLgel 10 μm mixed B column at a flow rate of 1 ml/min using tetrahydrofuran (THF) as a mobile phase. The M_n and M_w values were determined using the standard curve calibrated with a polystyrene standard. ^{1}H NMR spectroscopy was employed for the calculation of % molar grafting using a Bruker Avance 300 apparatus. Deuterated chloroform was used as a solvent, and the % molar grafting was calculated by the integrals of characteristic peaks in the ^{1}H NMR spectrum according to a published calculation method (Suksiriworapong et al., 2011). To investigate the polymorphism of the PEGylated copolymers, differential scanning calorimetry (DSC) was performed, and the DSC thermograms were recorded at the second heating run cycle at 20 °C/min over the temperature range of −80 °C to 100 °C.

2.3. Nanoparticle preparation of preformed PEGylated copolymers

The nanoparticles were prepared by a solvent diffusion and evaporation technique as reported elsewhere (Espuelas et al., 1997; Khoee et al., 2007). Firstly, a known amount of the preformed PEGylated copolymer was dissolved in 10 ml of THF. The polymeric solution (10 mg/ml) was then gently added into 16 ml of Milli-Q water under stirring at 1000 rpm. THF was evaporated under reduced pressure, and the final volume was readjusted to 16 ml. The obtained dispersion was filtered through 0.45 μm membrane filter (Millipore, Schwalbach, Germany) to eliminate aggregates. Finally, one milliliter of the nanoparticles was added into 2-ml vials and then frozen prior to freeze drying. The freeze dried powder of the nanoparticles was obtained after 48 h of freeze drying. The weight of the obtained powder was recorded. In case of drug loading, a preset amount of drug was initially dissolved together with the copolymer. The drug to polymer mass ratios (D:P) were set at 2:10 and 3:10. The drug-loaded nanoparticles were prepared as previously described.

2.4. Toxicity assay of PEGylated nanoparticles

The toxicity of the PEGylated nanoparticles was assessed by the MTT test using HUVECs. Cells were grown in IMDM culture medium containing 1% penicillin/streptomycin, 2% glutamine, 3% bicarbonate solution, 15% FBS, and 0.1% fibroblast growth factor. Cells (50 μl) at the density of 3×10^5 cells/ml were seeded into a 96-well plate and incubated in a 5% CO_2 atmosphere at 37 °C. After 24 h of incubation, the cells were incubated for another 24 h with an equal volume of the PEGylated nanoparticles dispersed in the culture medium. The final concentrations of the nanoparticles were varied in the range of 0.01–1.56 μg/ml. Subsequently, 25 μl of the MTT solution was added to each well. After 6 h of incubation, the cells were finally incubated with an SDS solution for 6 h. The % cell viability was calculated according to Eq. (1), and cells incubated without the nanoparticles were used as control.

$$\%\,\text{Cell viability} = \frac{A_{S,560} - A_{S,620}}{A_{C,560} - A_{C,620}} \times 100 \quad (1)$$

A_S and A_C denote the absorbance measured from the sample incubated with and without the nanoparticles, respectively. The numeric subscripts refer to the measurement wavelength.

2.5. Particle size and zeta potential measurements

The determination of the mean particle size (*z*-ave) and zeta potential (ZP) was performed by photon correlation spectroscopy (PCS) by means of a Zetasizer 3000 HSA (Malvern Instruments, Malvern, UK). All samples were diluted with Milli-Q water prior to measurement and measured with a HeNe laser at the wavelength of 633 nm, a 90° angle, and a temperature of 25 °C. All measurements were performed in triplicate.

2.6. Particle morphology

The samples were sputtered with gold (Agar Sputter Coater) for 45 s prior to measurement. The morphology of the nanoparticles was investigated by scanning electron microscopy (Hitachi S4500, Tokyo, Japan) equipped with a field-emissions-cathode using a 15 kV upper detector. The photograph was analysed using a

Digital Image Processing System 2.6 (Firma Point Electronic, Halle, Germany).

2.7. Drug loading and entrapment efficiency evaluation

The drug loading (% DL) and the entrapment efficiency (% EE) were evaluated by direct and indirect methods as reported earlier (Avgoustakis et al., 2002; Kisich et al., 2007). For the indirect procedure, the amount of drug in the filtrate was analysed after centrifugal filtration at 16,000 rpm using a Microcon Ultracel YM-30 tube (MWCO 30,000 Da) (Millipore, Schwalbach, Germany). For the direct method, the amount of drug in the dispersion was directly analysed after fresh preparation. The nanoparticles were dissolved in a mobile phase and sonicated for 30 min. Then the precipitate was centrifuged at 16,000 rpm for 10 min. The supernatant was collected and analysed by HPLC. The amount of drug entrapped in the nanoparticles was calculated from the different amounts of drug obtained by the direct and the indirect methods. Yield, entrapment efficiency and drug loading were calculated according to the following equations.

$$\%\,\text{Yield} = \frac{\text{Weight of freeze dried nanoparticles}}{\text{Initial weight of solid content}} \times 100 \quad (2)$$

$$\%\,\text{EE} = \frac{\text{Amount of entrapped drug in nanoparticles}}{\text{Amount of drug fed initially}} \times 100 \quad (3)$$

$$\%\,\text{DL} = \frac{\text{Amount of entrapped drug in nanoparticles}}{\text{Weight of freeze dried nanoparticles}} \times 100 \quad (4)$$

The weight of the freeze dried nanoparticles in Eq. (4) was the difference between the actual weight of freeze dried powder and the amount of non-entrapped drug presented in the filtrate as determined by the indirect method.

2.8. In vitro drug release study

The release study was performed by dialysis as reported elsewhere (Avgoustakis et al., 2002; Zhang and Zhuo, 2005). Briefly, 2.0 ml of the drug loaded nanoparticles were enclosed in a dialysis tube (MWCO, 6000–8000 Da, Bioron GmbH, Ludwigschafen, Germany). It was then immersed in phosphate buffer solution pH 7.4 used as a receptor medium. The experiment was performed at 37 °C under magnetic stirring at 130 rpm. At predetermined times, 0.5 ml of aliquot was withdrawn, and then the amount of drug released was analysed by the HPLC method as described below. After sampling, an equal volume of fresh medium was immediately added.

2.9. HPLC analysis

The quantitative analysis of drug was conducted by HPLC (LaChrom, Tokyo, Japan) equipped with a diode array detector (LaChrom model L-7455). IBU and IND were eluted through a reverse phase Hypersil ODS column, 5 μm particle size, 250 mm × 4.6 mm (Thermo Scientific, USA) at flow rates of 1.4 and 1.2 ml/min, respectively. The mixture of methanol: water: acetonitrile: acetic acid (55:35:10:1) was used as a mobile phase. The amount of IBU was calculated at the wave length of 264 nm using a standard curve over the range of 2.5–40 μg/ml, while that of IND was performed at 254 nm using a standard curve over the range of 0.25–40 μg/ml. The injection volume was 20 μl.

2.10. FT-IR measurement

The interaction between drug and PEGylated copolymer was evaluated by FT-IR spectroscopy. The samples were prepared by dissolving in THF. One drop of the sample solution was spread on KBr disc and allowed to dry in a desiccator. The measurement was conducted using a Nicolet 6700 FT/IR spectrophotometer (Thermo Fisher Scientific Inc., Massachusetts, USA). The absorption spectra of drug, NI grafted copolymer, and the mixture between drug and NI grafted copolymer were recorded.

2.11. Statistical analysis

Results are depicted as mean ± S.D. of at least three measurements. The *t*-test or one way ANOVA applied post hoc for paired comparisons were performed to compare two or multiple groups, respectively. All analyses were determined using the SPSS program (SPSS 13.0 for windows), and differences were considered to be significant at a level of p-value < 0.05. To compare the release profiles, a similarity factor (f_2) was calculated according to Eq. (5)

$$f_2 = 50 \log \left\{ \left[1 + 1/n \sum_{t=1}^{n} |R_1 - R_2|^2 \right]^{-0.5} \times 100 \right\} \quad (5)$$

where n is the number of time point. R_1 and R_2 represent the percent drug released of the sample 1 and 2 at each time point, t. Generally, f_2 values between 50 and 100 ensure that the two release profiles are similar (United States Food and Drug Administration, 1997).

3. Results and discussion

3.1. Preformed PEGylated copolymers

In accordance with our previously published method (Suksiriworapong et al., 2011), NI grafted $(PCL)_2$-PEG copolymers were obtained using the "click reaction". All molecular characteristics of PEGylated copolymers are summarized in Table 1. The molecular weight of PEGylated copolymers decreased with increasing % molar grafting whereas the M_w/M_n values were not different among all PEGylated copolymers. Previously, it was reported that the decrease in molecular weight could be attributed to inter- and intra-molecular transesterifications at high temperatures around 120 °C caused by a high reactive chloride atom of the monomer used in the polymerization, and a slight degradation of 30%$(P(NICL))_2$-PEG that is revealed by a small shoulder peak in the GPC chromatrogram (data not shown) (Suksiriworapong et al., 2010a, 2011). The glass transition temperature (T_g) of PEGylated copolymers tended to increase, whereas the melting temperature (T_m) and the enthalpy of melting (ΔH_m) decreased with increasing % molar grafting. The DSC results and thermograms (Fig. 1)

Table 1
Molecular characteristics of preformed PEGylated copolymers.

Copolymers	% Molar grafting[a]	$M_{n,GPC}$[b]	M_w/M_n[b]	T_g (°C)	T_m (°C)	ΔH_m (J/g)
$(PCL)_2$-PEG	0	9206	1.65	−60	54	47.7
10%$(P(NICL))_2$-PEG	9	7775	1.54	−50	40	45.8
20%$(P(NICL))_2$-PEG	17	6294	1.70	−47	39	17.6
30%$(P(NICL))_2$-PEG	25	5980	1.56	−43	32	5.5

[a] Determined by ^{1}H NMR spectroscopy.
[b] Determined by GPC.

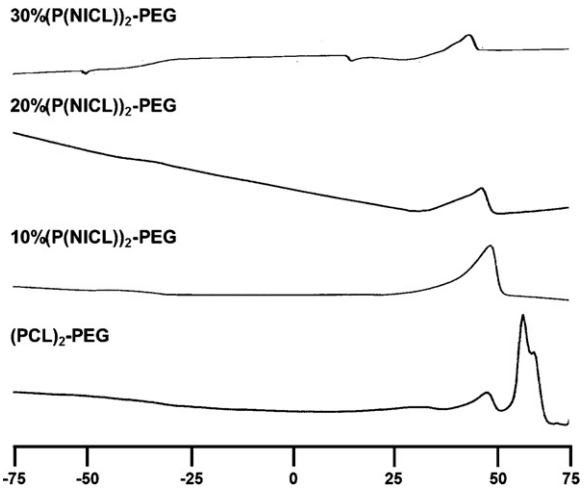

Fig. 1. DSC thermograms of $(PCL)_2$-PEG and $(P(NICL))_2$-PEG copolymers.

suggested that grafting with NI tended to reduce the crystalline properties of PEGylated copolymers.

3.2. Unloaded nanoparticles of preformed PEGylated copolymers

All $(P(NICL))_2$-PEG copolymers were further used for nanoparticle preparation. The $(PCL)_2$-PEG nanoparticles were used as a comparison. The characteristics of the unloaded nanoparticles are shown in Table 2. After using the solvent diffusion and evaporation method, the percent yield of all unloaded nanoparticles was higher than 78%. All $(P(NICL))_2$-PEG nanoparticles were smaller than the $(PCL)_2$-PEG nanoparticles, and their particle size increased with the increasing % molar grafting. The increasing % molar grafting increased the hydrophobic properties of PEGylated copolymers, thus increasing the particle size of nanoparticles (Shin et al., 1998; Jones and Leroux, 1999; Zhang et al., 2006b). The ZP of $(P(NICL))_2$-PEG nanoparticles was higher than that of $(PCL)_2$-PEG nanoparticles suggesting that the grafting NI component may be presented on the surface of the nanoparticles. The unloaded $(P(NICL))_2$-PEG nanoparticles were almost spherical in shape as shown in Fig. 2.

3.3. Toxicity assay of PEGylated nanoparticles

The toxicity results are illustrated in Table 2 and expressed as TC_{80} representing the toxic concentration of nanoparticles of less than 80% of cell viability. As illustrated, the TC_{80} values decreased with the increasing % molar grafting. The results indicated that an increase in % molar grafting NI increased the toxicity of the PEGylated copolymer nanoparticles. Owing to many factors determining the cytotoxicity of nanoparticles such as PEG surface density and particle size etc. (Gref et al., 1995; Stolnik et al., 1995; Allen et al., 1999; Mosqueira et al., 2001; Hu et al., 2007), the actual mechanism of cell death by the grafted nanoparticles could not be elucidated.

3.4. Drug loaded nanoparticles of preformed PEGylated copolymers

IBU and IND were chosen as model drugs to investigate the effect of grafting NI on the drug loading capacity. Table 3 combines % yield and % EE of the IBU- and IND-loaded nanoparticles. The yield of all drug-loaded nanoparticles was higher than 70%. At least 67% of IBU was entrapped in the nanoparticles. IND was entrapped in $(PCL)_2$-PEG and $(P(NICL))_2$-PEG nanoparticles to a significantly higher extent than IBU (p-value < 0.05) except for $(PCL)_2$-PEG nanoparticles loaded at a ratio of 3:10. The higher % EE of IND could be attributed to the lower water-solubility of IND as compared to IBU (Jiang et al., 2005; Zhang et al., 2006a). During the nanoparticle formation, the IND molecules were dissolved to a lower extent in water and hence partitioned more into hydrophobic core. This result is consistent with the previous report on the

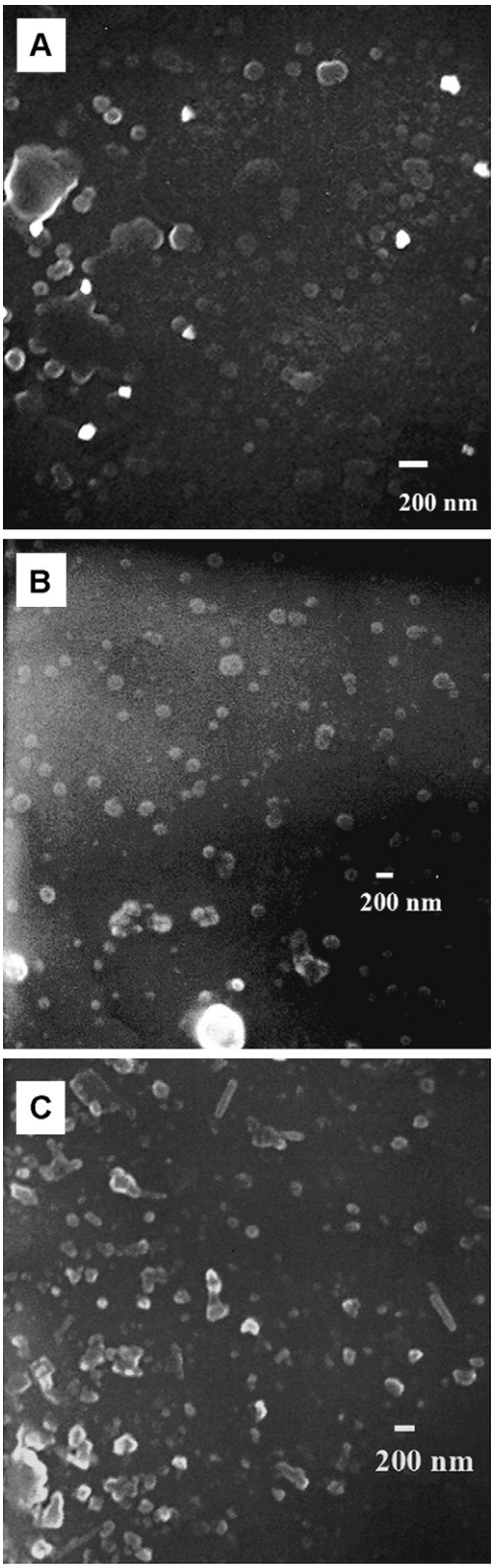

Fig. 2. Scanning electron microscopic photographs of unloaded $(P(NICL))_2$-PEG nanoparticles containing 10% (A), 20% (B), and 30% (C) molar grafting.

Table 2
Characteristics of unloaded PEGylated nanoparticles.

Copolymers	*z*-ave[a] (nm)	ZP[a] (mV)	% Yield	TC_{80}[b] (mg/ml)
$(PCL)_2$-PEG	123 ± 26	−3.7 ± 3.1	78.9 ± 8.6	1.56
10%$(P(NICL))_2$-PEG	77 ± 10	−8.9 ± 1.5	94.2 ± 0.0	0.78
20%$(P(NICL))_2$-PEG	82 ± 8	−5.9 ± 1.4	94.0 ± 4.5	0.78
30%$(P(NICL))_2$-PEG	120 ± 25	−17.3 ± 2.0	87.6 ± 1.1	0.39

The values are expressed as the mean ± S.D. from at least three experiments.
[a] *z*-ave = mean particle size, ZP = zeta potential.
[b] Toxic concentration of nanoparticles caused less than 80% of cell viability.

Table 3
% Yield and % entrapment efficiency (% EE) of drug-loaded nanoparticles.

Copolymers	D:P[a]	Drug			
		IBU		IND	
		% Yield	% EE	% Yield	% EE
$(PCL)_2$-PEG	2:10	80.9 ± 2.8	67.4 ± 11.4	89.0 ± 2.8	97.4 ± 14.7
	3:10	72.3 ± 2.6	69.9 ± 14.8	77.1 ± 2.6	47.2 ± 0.1
10%$(P(NICL))_2$-PEG	2:10	85.9 ± 1.0	73.2 ± 2.1	90.3 ± 2.8	87.6 ± 11.6
	3:10	94.8 ± 2.6	79.7 ± 2.2	92.0 ± 2.6	100.1 ± 0.2
20%$(P(NICL))_2$-PEG	2:10	94.1 ± 0.9	83.7 ± 2.1	92.3 ± 3.7	85.9 ± 10.0
	3:10	90.2 ± 2.6	78.2 ± 1.2	86.3 ± 1.7	82.5 ± 0.6
30%$(P(NICL))_2$-PEG	2:10	89.6 ± 2.9	78.2 ± 2.2	92.7 ± 4.7	93.1 ± 0.2
	3:10	98.0 ± 0.0	81.2 ± 1.7	92.1 ± 3.4	88.6 ± 0.7

The values are expressed as the mean ± S.D. from at least three experiments.
[a] Drug to polymer mass ratio.

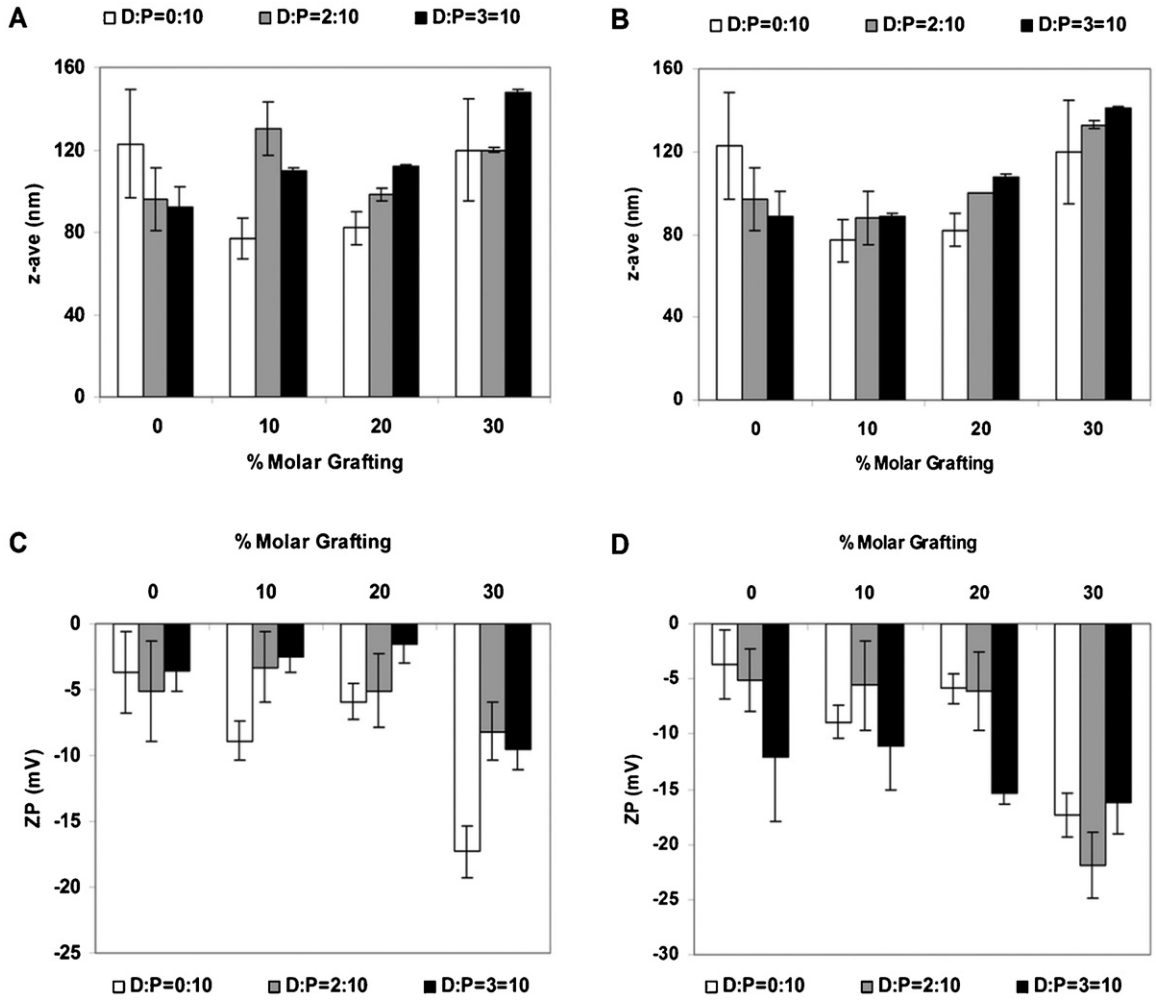

Fig. 3. *Z*-ave (A and B) and zeta potential (C and D) of IBU- (left panel) and IND- (right panel) loaded nanoparticles. Each point represents the mean ± S.D. of three experiments. D:P denotes drug to polymer mass ratio.

comparison of entrapment efficiency of loaded drugs having different water solubilities (Barichello et al., 1999; Corrigan and Li, 2009; Suksiriworapong et al., 2010b). In the case of IND-loaded $(PCL)_2$-PEG nanoparticles at 3:10, the dramatic reduction of the % EE could be due to the limitation of the system. The % EE of both drugs increased by incorporation into the NI grafted copolymer nanoparticles, particularly at D:P of 3:10 (p-value < 0.05), probably as the result of the increase in the hydrophobicity of the grafted copolymer. Fig. 3 demonstrates z-ave and ZP values of drug loaded nanoparticles. After incorporation of both drugs into $(P(NICL))_2$-PEG nanoparticles, most formulations showed larger particle sizes compared to the unloaded nanoparticles. The ZP of IBU-loaded $(P(NICL))_2$-PEG nanoparticles tended to increase while that of IND-loaded nanoparticles showed the opposite result. However, no relation between ZP and amount of loaded drug was evidenced. Fig. 4 shows that increasing amounts of loaded drug increased the % DL of both drugs in $(P(NICL))_2$-PEG nanoparticles. In addition, the nanoparticles containing grafting NI revealed a higher % DL as compared to those without grafting except for IND loaded at 2:10. However, the increasing % molar grafting did not significantly correlate to % DL. It could be deducted that the presence of grafting NI enhanced the loading capacity of $(PCL)_2$-PEG nanoparticles presumably due to the enhanced hydrophobic properties of the grafted copolymers. The drug-loaded $(P(NICL))_2$-PEG nanoparticles remained spherical in shape as exemplified in Fig. 5.

3.5. In vitro drug release

In the present experiments, the nanoparticles containing 10% and 20% molar grafting NI and loading with drug at D:P of 2:10 were chosen for the release study in comparison with $(PCL)_2$-PEG nanoparticles. Fig. 6 displays the release profiles of drug-loaded nanoparticles. The data from the release curves of all nanoparticles indicated a linear relationship following the Higuchi model (Higuchi, 1963), as seen in Fig. 7. All release profiles could be fitted to the Higuchi model over the initial 4 h of the release with $r^2 > 0.941$ indicating Fickian diffusion. In the case of $(PCL)_2$-PEG nanoparticles, about 80% of both drugs was released over 24 h (Fig. 6). The release profile and release rate of IND were not different to those of IBU (f_2 value of release profile = 63.5 and p-value of release rate > 0.05). It was expected that the less water-soluble drug, IND, would be released slower and to a lower extent than the higher water-soluble drug, IBU, from the same nanocarrier. However, the release rate and amount of drug release depended on the surface area and the initial drug concentration in the system. Since the particle sizes of both drug-loaded $(PCL)_2$-PEG nanoparticles

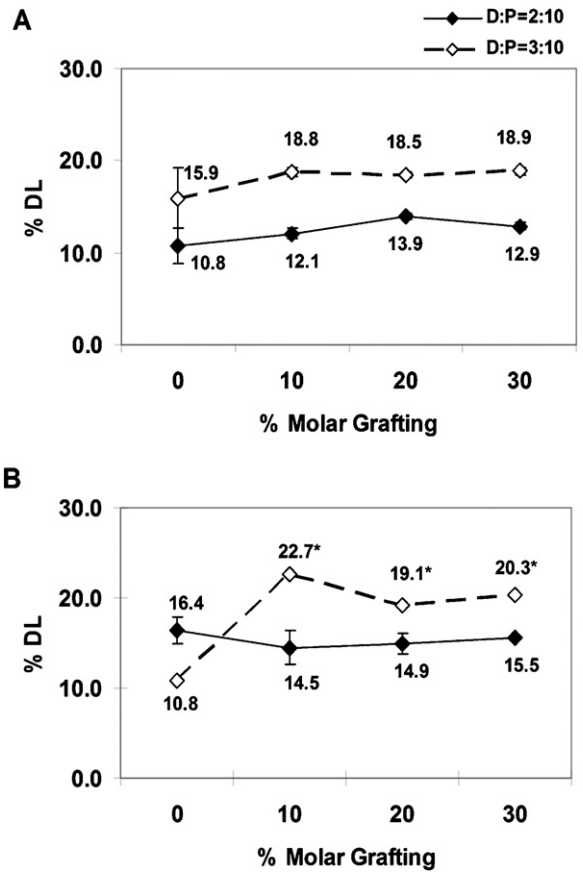

Fig. 4. Relationship of % drug loading (% DL) and % molar grafting of IBU- (A) and IND- (B) loaded nanoparticles. Each point represents the mean ± S.D. of three experiments. D:P denotes drug to polymer mass ratio (*Statistically significant difference compared with 0% molar grafting $(PCL)_2$-PEG nanoparticles (p-value < 0.05)).

were not significantly different indicating similar surface areas, the insignificant difference in the release rate and profile between IND and IBU probably can be attributed to the significantly higher % DL of IND. Therefore, the higher % DL thus enhanced the drug released from the carrier although IBU possesses higher water-solubility than IND as already mentioned (Barichello et al., 1999; Corrigan and Li, 2009).

For $(P(NICL))_2$-PEG nanoparticles, the release profile and rate of IBU from 20%$(P(NICL))_2$-PEG nanoparticles (Figs. 6A and 7A)

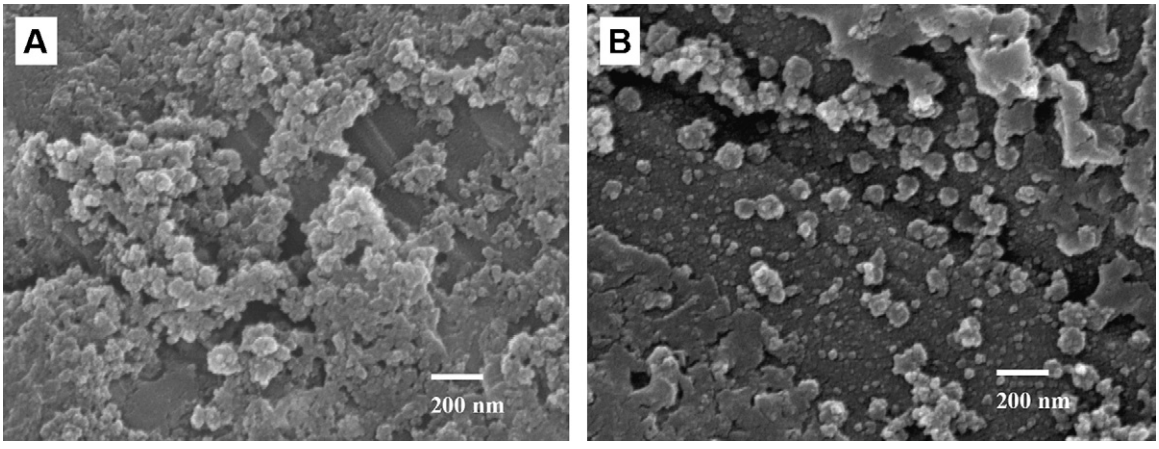

Fig. 5. Scanning electron microscopic photographs of IBU- (A) and IND- (B) loaded 10%$(P(NICL))_2$-PEG nanoparticles at D:P of 2:10.

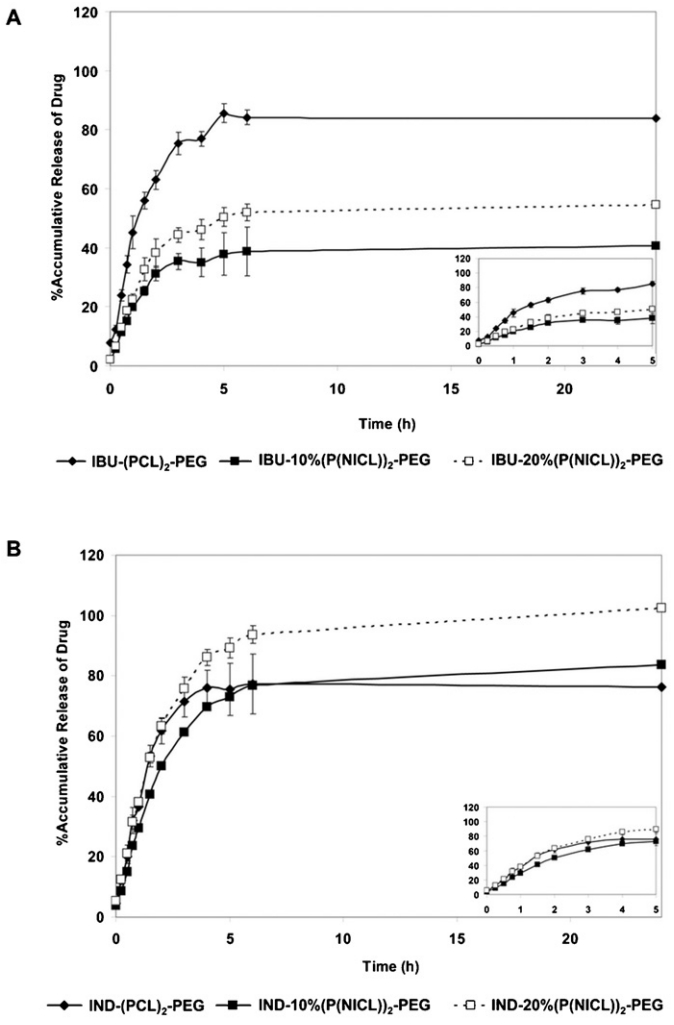

Fig. 6. Release profiles of IBU- (A) and IND- (B) loaded nanoparticles in phosphate buffer solution pH 7.4 at 37 °C over 24 h. Drug to polymer mass ratio was 2:10. Each point represents the mean ± S.D. of three experiments. The insets show the release profiles during the initial 5 h of release.

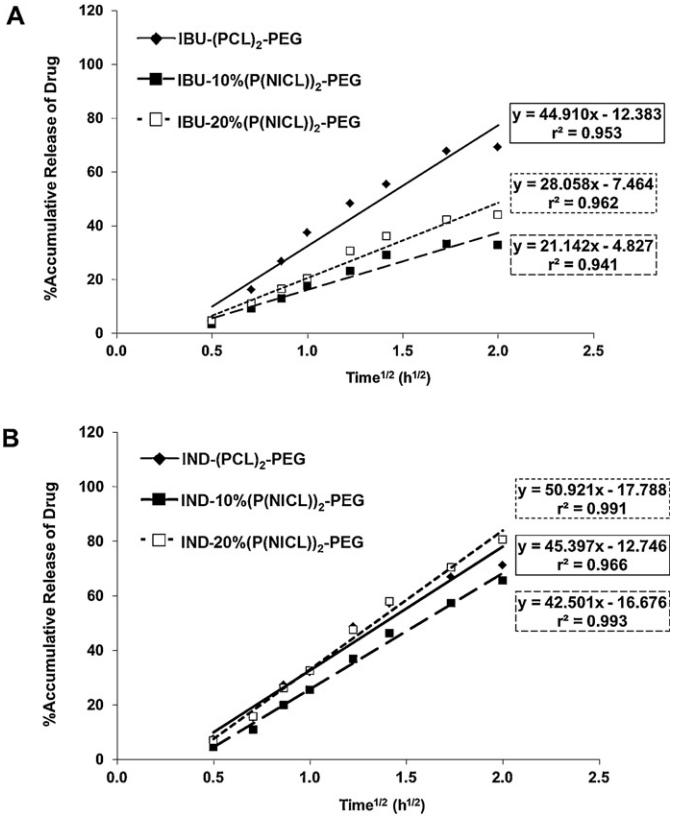

Fig. 7. Higuchi model fitting of the in vitro IBU (A) and IND (B) release profiles from nanoparticles during the initial 4 h of the release.

were not different than those of 10%(P(NICL))$_2$-PEG nanoparticles (f_2 value = 53.5 and p-value > 0.05, respectively). The total release (Fig. 6B) and release rate (Fig. 7B) of IND from 20%(P(NICL))$_2$-PEG nanoparticles were higher than those of 10%(P(NICL))$_2$-PEG nanoparticles (f_2 value = 44.9 and p-value < 0.01, respectively) due to the lower crystalline properties of the grafted copolymer. It has been reported that the lower crystallinity of a copolymer facilitated the drug diffusing through the polymeric matrix of nanoparticles, thus enhancing drug release (Allen et al., 1999). The DSC results in Table 1 show that the melting enthalpy of 20%(P(NICL))$_2$-PEG was lower than that of 10%(P(NICL))$_2$-PEG. It was noticeable that the different release pattern of both drugs was affected by the characteristic of nanoparticles and crystalline properties of copolymers as a consequence of the increasing % molar grafting.

To compare the release profiles of IND and IBU, the release profiles and release rates of both drugs from 20%(P(NICL))$_2$-PEG nanoparticles were used since all other parameters were not significantly different. Particle sizes and % DL of the 20%(P(NICL))$_2$-PEG and the (PCL)$_2$-PEG nanoparticles were also not different. IBU showed definitely slower release rates (p-value < 0.001) and lower amounts released (f_2 value = 27.3) than IND despite its higher water-solubility. This may have resulted from the interaction between IBU and grafted NI documented in the FT-IR spectra (Fig. 8). The spectrum of IBU displayed a O—H stretching peak at 3495 cm^{-1} and a C=O stretching peak at 1733 cm^{-1}. The individual peaks of (P(NICL))$_2$-PEG were detected and assigned to the terminal O—H stretching at 3569 and 3499 cm^{-1}, a C=O stretching at 1733 cm^{-1}, and a C=N stretching at 1651 cm^{-1}. However, in the spectrum of the mixture of IBU and (P(NICL))$_2$-PEG, the O—H stretching region of both, IBU and (P(NICL))$_2$-PEG, was shifted to 3445 cm^{-1}. The band at 1651 cm^{-1} was not detected with the presence of the new peak at 1736 cm^{-1}. This result suggested that the change in the frequency and pattern of the FT-IR spectra could be assigned to the hydrogen bonding between the O—H group of IBU and either the pyridinyl, triazolyl, or carbonyl group of (P(NICL))$_2$-PEG backbone. On the contrary, no alteration in the frequency and pattern in FT-IR spectrum of the mixture of IND and (P(NICL))$_2$-PEG was observed. Obviously the grafting NI affected the extent and rate of release of drug depending on the interactions between the drug and the copolymer.

In the case of IBU (Figs. 6A and 7A), the extent and rate of release from 20%(P(NICL))$_2$-PEG nanoparticles were markedly lower than those from (PCL)$_2$-PEG nanoparticles (f_2 value of 30.6 and p-value < 0.001, respectively) although the 20%(P(NICL))$_2$-PEG copolymer showed less crystalline property than the (PCL)$_2$-PEG copolymer. This result was due to the interaction between IBU and grafted copolymer. Therefore, it was confirmed that the interaction between IBU and grafted copolymer had larger effect on the drug release than the crystallinity of the copolymer. In contrast, in the case of IND due to the lower crystallinity of 20%(P(NICL))$_2$-PEG copolymer and the lack of interaction between IND and the copolymer, a slightly different release profile (Fig. 6B, f_2 value of 49.3) but an insignificantly higher release rate (Fig. 7B) of the 20%(P(NICL))$_2$-PEG nanoparticles resulted as compared to the (PCL)$_2$-PEG nanoparticles.

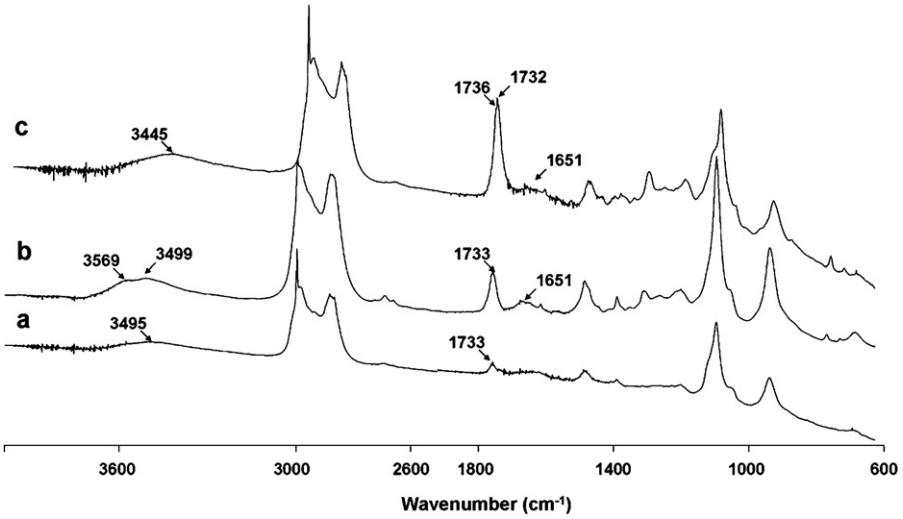

Fig. 8. FT-IR spectra of IBU (a), $(P(NICL))_2$-PEG (b), and the mixture of IBU and $(P(NICL))_2$-PEG (c).

4. Conclusion

This study showed that the grafting NI onto the polymer backbone affected both the nanoparticle formation and the characteristics of the nanoparticles. The amounts of grafting NI led to the increases in the hydrophobic properties of the copolymer and the mean particle size of the nanoparticles. The toxicity of nanoparticles increased with the increasing % molar grafting. Moreover, the grafting NI influenced the loading capacity and the release characteristics of the nanoparticles. The higher loading capacity of $(P(NICL))_2$-PEG nanoparticles in comparison to the $(PCL)_2$-PEG nanoparticles resulted from the presence of the grafting NI. The loading capacity additionally depended on the water solubility of the drug. Finally, differences in release characteristics of the nanoparticles could be contributed to (i) the mean particle size of the nanoparticles, (ii) the % DL of the nanoparticles, (iii) the crystalline properties of the copolymer, and (iv) the interaction between loaded drug and copolymer.

Acknowledgements

The authors gratefully acknowledge the Thailand Research Fund (TRF) through the Royal Golden Jubilee Ph.D. Program (Grant No. PHD/0189/2547) and the Thai Research Fund and Commission of Higher Education, Thailand for the research funding (RMU5180019) for the financial supports. The authors are very pleased to thank the National Metal and Materials Technology Center (MTEC, Pathumthani, Thailand) for the GPC experiment and Denise Klassert, Frankfurter Stiftung für Krebskranke Kinder, Frankfurt am Main, Germany, for assistance with the cytotoxicity study.

References

Alexis, F., Pridgen, E., Molnar, L.K., Farokhzad, O.C., 2008. Factors affecting the clearance and biodistribution of polymeric nanoparticles. Mol. Pharmacol. 5, 505–515.

Allen, C., Maysinger, D., Eisenberg, A., 1999. Nano-engineering block copolymer aggregates for drug delivery. Colloids Surf. B Biointerfaces 16, 3–27.

Avgoustakis, K., Beletsi, A., Panagi, Z., Klepetsanis, P., Karydas, A.G., Ithakissios, D.S., 2002. PLGA-mPEG nanoparticles of cisplatin: in vitro nanoparticle degradation, in vitro drug release and in vivo drug residence in blood properties. J. Control. Release 79, 123–135.

Barichello, J.M., Morishita, M., Takayama, K., Nagai, T., 1999. Encapsulation of hydrophilic and lipophilic drugs in PLGA nanoparticles by the nanoprecipitation method. Drug Dev. Ind. Pharm. 25, 471–476.

Chausson, M., Fluchére, A.-S., Landreau, E., Aguni, Y., Chevalier, Y., Hamaide, T., Abdul-Malak, N., Bonnet, I., 2008. Block copolymers of the type poly(caprolactone)-b-poly(ethylene oxide) for the preparation and stabilization of nanoemulsions. Int. J. Pharm. 362, 153–162.

Corrigan, O.I., Li, X., 2009. Quantifying drug release from PLGA nanoparticulates. Eur. J. Pharm. Sci. 37, 477–485.

Espuelas, M.S., Legrand, P., Irache, J.M., Gamazo, C., Orecchioni, A.M., Devissaguet, J.P., Ygartua, P., 1997. Poly(ε-caprolactone) nanospheres as an alternative way to reduce amphotericin B toxicity. Int. J. Pharm. 158, 19–27.

Gou, M., Zheng, L., Peng, X., Men, K., Zheng, X., Zeng, S., Guo, G., Luo, F., Zhao, X., Chen, L., Wei, Y., Qian, Z., 2009. Poly(ε-caprolactone)-poly(ethylene glycol)-poly(ε-caprolactone) (PCL-PEG-PCL) nanoparticles for honokiol delivery in vitro. Int. J. Pharm. 375, 170–176.

Gref, R., Domb, A., Quellec, P., Blunk, T., Müller, R.H., Verbavatz, J.M., Langer, R., 1995. The controlled intravenous delivery of drugs using PEG-coated sterically stabilized nanospheres. Adv. Drug Deliv. Rev. 16, 215–233.

Higuchi, T., 1963. Mechanism of sustained-action medication. Theoretical analysis of rate of release of solid drugs dispersed in solid matrices. J. Pharm. Sci. 52, 1145–1149.

Hu, Y., Jiang, X., Ding, Y., Zhang, L., Yang, C., Zhang, J., Chen, J., Yang, Y., 2003. Preparation and drug release behaviors of nimodipine-loaded poly(caprolactone)-poly(ethylene oxide)-polylactide amphiphilic copolymer nanoparticles. Biomaterials 24, 2395–2404.

Hu, Y., Xie, J., Tong, Y.W., Wang, C.-H., 2007. Effect of PEG conformation and particle size on the cellular uptake efficiency of nanoparticles with the HepG2 cells. J. Control. Release 118, 7–17.

Huang, M.J., Gou, M.L., Qian, Z.Y., Dai, M., Li, X.Y., Cao, M., Wang, K., Zhao, J., Yang, J.L., Lu, Y., Tu, M.J., Wei, Y.Q., 2008. One-step preparation of poly(ε-caprolactone)-poly(ethylene glycol)-poly(ε-caprolactone) nanoparticles for plasmid DNA delivery. J. Biomed. Mater. Res. A 86, 979–986.

Jiang, B., Hu, L., Gao, C., Shen, J., 2005. Ibuprofen-loaded nanoparticles prepared by a co-precipitation method and their release properties. Int. J. Pharm. 304, 220–230.

Jones, M.-C., Leroux, J.-C., 1999. Polymeric micelles – a new generation of colloidal drug carriers. Eur. J. Pharm. Biopharm. 48, 101–111.

Khoee, S., Hassanzadeh, S., Goliaie, B., 2007. Effects of hydrophobic drug–polyesteric core interactions on drug loading and release properties of poly(ethylene glycol)–polyester–poly(ethylene glycol) triblock core–shell nanoparticles. Nanotechnology 18, 175602.

Kisich, K.O., Gelperina, S., Higgins, M.P., Wilson, S., Shipulo, E., Oganesyan, E., Heifets, L., 2007. Encapsulation of moxifloxacin within poly(butyl cyanoacrylate) nanoparticles enhances efficacy against intracellular *Mycobacterium tuberculosis*. Int. J. Pharm. 345, 154–162.

Lee, J., Cho, E.C., Cho, K., 2004. Incorporation and release behavior of hydrophobic drug in functionalized poly(D,L-lactide)-block-poly(ethylene oxide) micelles. J. Control. Release 94, 323–335.

Lee, J.S., Hwang, S.J., Lee, D.S., 2009. Formation of poly(ethylene glycol)-poly(ε-caprolactone) nanoparticles via nanoprecipitation. Macromol. Res. 17, 72–78.

Liu, J., Xiao, Y., Allen, C., 2004. Polymer-drug compatibility: a guide to the development of delivery systems for the anticancer agent, ellipticine. J. Pharm. Sci. 93, 132–143.

Lou, X., Detrembleur, C., Jerome, R., 2003. Novel aliphatic polyesters based on functional cyclic (di)esters. Macromol. Rapid Commun. 24, 161–172.

Mosqueira, V.C., Legrand, P., Morgat, J.L., Vert, M., Mysiakine, E., Gref, R., Devissaguet, J.P., Barratt, G., 2001. Biodistribution of long-circulating PEG-grafted nanocapsules in mice: effects of PEG chain length and density. Pharm. Res. 18, 1411–1419.

Nair, R., Nyamweya, N., Gönen, S., Martínez-Miranda, L.J., Hoag, S.W., 2001. Influence of various drugs on the glass transition temperature of poly(vinylpyrrolidone): a thermodynamic and spectroscopic investigation. Int. J. Pharm. 225, 83–96.

Nguyen, T.H.A., Nguyen, V.C., 2010. Formation of nanoparticles in aqueous solution from poly(ε-caprolactone)-poly(ethylene glycol)-poly(ε-caprolactone). Adv. Nat. Sci.: Nanosci. Nanotechnol. 1, 025012.

Peng, C.-L., Shieh, M.-J., Tsai, M.-H., Chang, C.-C., Lai, P.-S., 2008. Self-assembled star-shaped chlorin-core poly(ε-caprolactone)-poly(ethylene glycol) diblock copolymer micelles for dual chemo-photodynamic therapies. Biomaterials 29, 3599–3608.

Riva, R., Lussis, P., Lenoir, S., Jérôme, C., Jérôme, R., Lecomte, P., 2008. Contribution of click chemistry to the synthesis of antimicrobial aliphatic copolyester. Polymer 49, 2023–2028.

Sarisuta, N., Kumpugdee, M., Müller, B.W., Puttipipatkhachorn, S., 1999. Physicochemical characterization of interactions between erythromycin and various film polymers. Int. J. Pharm. 186, 109–118.

Shenoy, D.B., Amiji, M.M., 2005. Poly(ethylene oxide)-modified poly(ε-caprolactone) nanoparticles for targeted delivery of tamoxifen in breast cancer. Int. J. Pharm. 293, 261–270.

Shin, G.I., Kim, Y.S., Lee, M.Y., Cho, S.C., Kiel, Y.S., 1998. Methoxypoly(ethylene glycol)/ε-caprolactone amphiphilic block copolymeric micelle containing indomethacin. I. Preparation and characterization. J. Control. Release 51, 1–11.

Simon, L.S., 2002. Nonsteroidal antiinflamatory drugs and cyclooxygenase-2 selective inhibitors. In: Smith, H.S. (Ed.), Drugs For Pain. Hanley & Belfus, Inc., Philadelphia, pp. 41–54.

Sinko, P.J., 2006. Biomaterials. In: Sinko, P.J. (Ed.), Martin's Physical Pharmacy and Pharmaceutical Sciences: Physical, Chemical and Biopharmaceutical Principles in the Pharmaceutical Sciences. Lippincott Williams & Wikins, Baltimore, pp. 585–627.

Stolnik, S., Illum, L., Davis, S.S., 1995. Long circulating microparticulate drug carriers. Adv. Drug Deliv. Rev. 16, 195–214.

Suksiriworapong, J., Sripha, K., Junyaprasert, V.B., 2010a. Synthesis and characterization of bioactive molecules grafted on poly(ε-caprolactone) by click chemistry. Polymer 51, 2286–2295.

Suksiriworapong, J., Sripha, K., Kreuter, J., Junyaprasert, V.B., 2010b. Comparative study of ibuprofen and indomethacin loaded poly(caprolactone) nanoparticles: physicochemical properties. Mahidol J. Pharm. Sci. 37, 17–27.

Suksiriworapong, J., Sripha, K., Kreuter, J., Junyaprasert, V.B., 2011. Investigation of polymer and nanoparticle properties with nicotinic acid and *p*-aminobenzoic acid grafted on poly(ε-caprolactone)-poly(ethylene glycol)-poly(ε-caprolactone) via click chemistry. Bioconjug. Chem. 22, 582–594.

Trollsas, M., Lee, V.Y., Mecerreyes, D., Lowenhielm, P., Moller, M., Miller, R.D., Hedrick, J., 2000. Hydrophilic aliphatic polyesters: design, synthesis, and ring-opening polymerization of functional cyclic esters. Macromolecules 33, 4619–4627.

United States Food and Drug Administration, 1997. Guidance for Industry: Dissolution Testing of Immediate Release Solid Oral Dosage Forms. U.S. Department of Health and Human Services Food and Drug Administration Center for Drug Evaluation and Research (CDER) (accessed 01.09.11) http://www.fda.gov/cder/guidance/1713bp1.pdf.

Van Krevelen, D., TeNijehuis, K., 2009. Cohesive properties and solubility. In: Van Krevelen, D., TeNijehuis, K. (Eds.), Properties of Polymers – Their Correlation with Chemical Structure, Their Numerical Estimation and Prediction from Additive Group Contributions. Elsevier Science Publisher B.V., Amsterdam, pp. 189–227.

Vroman, B., Ferreira, I., Jerome, C., Jerome, R., Preat, V., 2007a. PEGylated quaternized copolymer/DNA complexes for gene delivery. Int. J. Pharm. 344, 88–95.

Vroman, B., Mazza, M., Fernandez, M.R., Jerome, R., Preat, V., 2007b. Copolymers of ε-caprolactone and quaternized ε-caprolactone as gene carriers. J. Control. Release 118, 136–144.

Wei, X., Gong, C., Gou, M., Fu, S., Guo, Q., Shi, S., Luo, F., Guo, G., Qiu, L., Qian, Z., 2009a. Biodegradable poly(ε-caprolactone)-poly(ethylene glycol) copolymers as drug delivery system. Int. J. Pharm. 381, 1–18.

Wei, X., Gong, C., Shi, S., Fu, S., Men, K., Zeng, S., Zheng, X., Gou, M., Chen, L., Qiu, L., Qian, Z., 2009b. Self-assembled honokiol-loaded micelles based on poly(ε-caprolactone)-poly(ethylene glycol)-poly(ε-caprolactone) copolymer. Int. J. Pharm. 369, 170–175.

Zhang, J.X., Li, X.J., Qiu, L.Y., Li, X.H., Yan, M.Q., Yi, J., Zhu, K.J., 2006a. Indomethacin-loaded polymeric nanocarriers based on amphiphilic polyphosphazenes with poly (N-isopropylacrylamide) and ethyl tryptophan as side groups: preparation, in vitro and in vivo evaluation. J. Control. Release 116, 322–329.

Zhang, L., Hu, Y., Jiang, X., Yang, C., Lu, W., Yang, Y.H., 2004. Camptothecin derivative-loaded poly(caprolactone-co-lactide)-b-PEG-b-poly(caprolactone-co-lactide) nanoparticles and their biodistribution in mice. J. Control. Release 96, 135–148.

Zhang, N., Guo, S.R., Li, H.Q., Liu, L., Li, Z.H., Gu, J.R., 2006b. Synthesis of three types of amphiphilic poly(ethylene glycol)-*block*-poly(sebacic anhydride) copolymers and studies of their micellar solutions. Macromol. Chem. Phys. 207, 1359–1367.

Zhang, Y., Zhuo, R.-X., 2005. Synthesis and in vitro drug release behavior of amphiphilic triblock copolymer nanoparticles based on poly (ethylene glycol) and polycaprolactone. Biomaterials 26, 6736–6742.

Zhou, S., Deng, X., Yang, H., 2003. Biodegradable poly(ε-caprolactone)-poly(ethylene glycol) block copolymers: characterization and their use as drug carriers for a controlled delivery system. Biomaterials 24, 3563–3570.